


## Article

# Oxyfuel Combustion of a Model MSW—An Experimental Study

Michaël Becidan <sup>1,\*</sup>, Mario Ditaranto <sup>1</sup> , Per Carlsson <sup>1</sup>, Jørn Bakken <sup>1</sup>, Maria N. P. Olsen <sup>1</sup> and Johnny Stuen <sup>2</sup>

<sup>1</sup> Department of Thermal Energy, SINTEF Energy Research, 7465 Trondheim, Norway; mario.ditaranto@sintef.no (M.D.); per.carlsson@vowasa.com (P.C.); jorn.bakken@sintef.no (J.B.); maria.olsen@sintef.no (M.N.P.O.)

<sup>2</sup> Agency for Waste Management (REG), City of Oslo, 0516 Oslo, Norway; johnny.stuen@reg.oslo.kommune.no

\* Correspondence: michael.becidan@sintef.no

**Abstract:** The oxyfuel combustion of a model MSW (municipal solid waste) under various conditions was carried out in a lab-scale reactor. The aim was to study the behavior of MSW and identify challenges and opportunities associated with the development of this technology in the context of integration with CCS (carbon capture and storage). The experimental results show the effects of the oxidizer composition on the combustion process. Complete combustion can be attained under a variety of oxyfuel conditions, and the differences highlighted with O<sub>2</sub>/CO<sub>2</sub> as an oxidizer compared with O<sub>2</sub>/N<sub>2</sub> do not constitute showstoppers. MSW oxyfuel combustion hence offers a great potential for the combined (1) treatment of waste (contaminants' destruction, volume, and weight reduction), (2) production of heat/power, and (3) CCS with negative CO<sub>2</sub> emissions.

**Keywords:** oxyfuel combustion; oxygen-enhanced combustion (OEC); municipal solid waste (MSW); waste-to-energy (WtE); biomass; BECCS/bioCCS (Bioenergy carbon capture and storage); GHG (greenhouse gases); climate change; gaseous emissions; FTIR (Fourier-transform infrared) analyzer



**Citation:** Becidan, M.; Ditaranto, M.; Carlsson, P.; Bakken, J.; Olsen, M.N.P.; Stuen, J. Oxyfuel Combustion of a Model MSW—An Experimental Study. *Energies* **2021**, *14*, 5297. <https://doi.org/10.3390/en14175297>

Academic Editor: Adonios Karpetsis

Received: 1 July 2021

Accepted: 23 August 2021

Published: 26 August 2021

**Publisher's Note:** MDPI stays neutral with regard to jurisdictional claims in published maps and institutional affiliations.



**Copyright:** © 2021 by the authors. Licensee MDPI, Basel, Switzerland. This article is an open access article distributed under the terms and conditions of the Creative Commons Attribution (CC BY) license (<https://creativecommons.org/licenses/by/4.0/>).

## 1. Introduction

Municipal solid waste (MSW) is a complex mixture produced by households as well as commercial and service activities. The current treatment and disposal methods include landfilling, material recycling (especially for metals, glass, paper products, and plastics) and energy recovery in waste-to-energy (WtE) plants. Composting and biogas production (via anaerobic digestion) are also employed for biodegradable waste fractions. Sadly, adequate waste management is only widespread in parts of Europe, North America, and Asia. Worldwide, an estimated 70% of the solid waste is dumped in uncontrolled dumps or landfills, causing an array of hygienic and environmental problems, including uncontrolled CH<sub>4</sub> emissions, a highly potent GHG (Greenhouse Gas) [1]. With an increasing population, improving standards of living for many as well as stronger environmental awareness can only mean that more MSW will be produced in the future, but also that both material recycling and WtE capacities will have to increase on a massive scale.

The development soon-to-be impacting the waste management sector is related to climate change and GHG emissions. The Intergovernmental Panel on Climate Change (IPCC) scenarios [2] modelled for Earth's climate evolution in the coming decades show that the Paris' agreement ambitious goals to mitigate temperature increase can only be met with carbon capture and storage (CCS), and, in all probabilities, solutions allowing for negative CO<sub>2</sub> emissions, in other words, removing CO<sub>2</sub> from the atmosphere. With MSW being mainly biogenic, more than 50% in most European cases [3], CCS integrated with WtE can be a viable CO<sub>2</sub> negative alternative in addition to BECCS (Bioenergy carbon capture and storage).

How can CCS be applied to WtE? The main characteristics of WtE are rather different from oil/gas/coal-fired power/heat generation systems, for which CCS has been largely developed. The vast majority of WtE plants in the world are grate-fired installations with a MSW throughput of approx. 200,000 tons per year per plant [3] (European average) and producing heat (district heat, processed heat for the industry) and/or power. Western MSW has a lower heating value of about 8–12 MJ/kg and is highly heterogeneous. It contains many minor and trace compounds not found in other solid fuels, and its properties will vary over time, both on a minute and season basis, making stable operation a challenge and limiting overall energy efficiency. Each ton of MSW produces about one ton of CO<sub>2</sub> during combustion. CO<sub>2</sub> concentrations in the flue gas are comparable to (wet basis) coal incineration, and a highly advanced flue gas treatment is required to meet emissions values limits. WtE plants are on average much smaller than coal-fired power plants, making downscaling and economy of scale an issue when considering CCS integration.

Despite these specific conditions, post-combustion CO<sub>2</sub> capture based on solvents such as amines appears to be promising, as demonstrated by the pilot testing performed by Fortum Oslo Varme in their WtE plant in Klemetsrud, Oslo, Norway [4]. However, for greenfield applications, innovative capture solutions can offer additional benefits. Oxyfuel combustion is combustion using pure oxygen or a mixture of oxygen and (recirculated) flue gas (i.e., mainly CO<sub>2</sub>) as an oxidizer instead of using air. In this context, the advantages of oxyfuel combustion for CCS are obvious: the exhaust gas is mainly composed of CO<sub>2</sub> that can easily be captured through water condensation and removal of impurities. The proposed technological combination (oxyfuel combustion + energy production + flue gas treatment + CCS) for a new generation of WtE plants will offer net negative CO<sub>2</sub> emissions + minimal emissions + energy recovery (heat and power from non-recyclables) + safe thermal waste treatment (sanitization, destruction of organic contaminants, reduction in volume and weight). This will make WtE an integral part of a more circular economy.

Oxyfuel combustion has so far been developed and demonstrated for coal [5], for which it has shown great potential. The use of pure oxygen in addition to air or full substitution for combustion in industrial processes has been known for many years [6] for its advantages in terms of higher temperature, lower flue gas volumes, and higher heat transfer rate, amongst others. In the context of MSW oxyfuel combustion integrated with CCS, it seems preferable to keep or modified as little as possible the main features of air-fired grate combustion to benefit from this robust technology experience and know-how. This would include keeping temperatures close to air combustion (especially in the combustion chamber) via flue gas recycling to avoid the need for expensive materials and alloys as well as prevent ash-related challenges such as slagging. However, only limited work has been performed on biomass and waste. The studies using coal have only limited relevance as these three fuels are fundamentally different. Key fundamental findings from oxyfuel combustion of coal include: (1) the oxyfuel combustion environment (N<sub>2</sub>, CO<sub>2</sub>) affects the combustion process (devolatilization and char burnout), e.g., the overall char burning rate is lower with CO<sub>2</sub> than with N<sub>2</sub> [7,8]; (2) to obtain flame stability and ignition similar to air, a O<sub>2</sub> concentration of 30 vol% is necessary in CO<sub>2</sub> [9]; (3) a general observation (but it cannot be generalized) is that NO<sub>x</sub> emissions are lower in oxyfuel combustion on an energy basis (mg/MJ) [10] but the NO<sub>x</sub> concentration (ppm or mg/Nm<sup>3</sup>) in the flue gas of oxy-combustion is usually similar or higher than that in air combustion [11].

As already mentioned, MSW is highly heterogeneous and contains high levels of moisture and ash, as well as several minor and trace elements not found in coal. Existing studies are focusing on extremely small-scale experiments (thermogravimetric analysis (TGA) for kinetics studies) of individual waste or biomass fractions or investigate the pyrolysis process as the first stage of combustion. Results concerning the combustion process and selected emissions have shown that oxyfuel combustion of MSW is worth exploring further [12]. Key findings on fundamental aspects (TGA of single waste fractions) are similar to coal's, e.g., the negative effects of CO<sub>2</sub> on flame stability and ignition [13], or

$\text{NO}_x$  emissions that are usually reported to decrease with oxy fuel combustion but not in all studies [14,15].

However, the topic requires more laboratory-scale (larger than TGA), well-controlled experimental studies with MSW-like mixtures, rather than individual homogeneous fractions and using advanced analytical measurements. It is especially interesting to explore several key aspects simultaneously in a continuous thermal conversion process, namely temperature, combustion stability, and emissions, as performed in this study.

In this work, we aim at demonstrating the feasibility of oxyfuel combustion with MSW using lab-scale experiments and discuss advantages as well as any showstopper for this technology in the context of CCS integration for WtE. We will carry out this work by comparing air and oxy-combustion characteristics for MSW at different conditions and determining the fundamental behavior of MSW during oxyfuel combustion.

## 2. Materials and Methods

### 2.1. Experimental Set-Up

Figure 1 shows the vertical tube furnace (VTF) reactor used in this study. It includes a 2000 mm long, 120 mm inner diameter tube, at the bottom of which a perforated grate is placed. The ceramic tube is surrounded by 3 separate electric heaters and insulation. Three thermocouples (T+287, T+672 and T+1152, the number indicating the distance from the grate in millimeters) placed as shown in the figure allow to monitor the temperature inside the reactor.

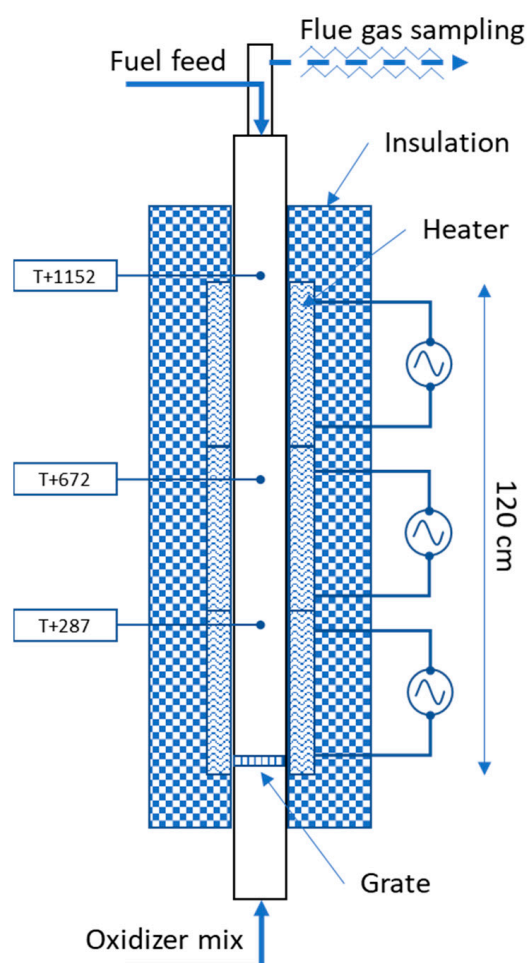


**Figure 1.** Sketch of the vertical tube furnace (VTF) reactor showing the three independently regulated heating zones, streams in and out, the grate, and the thermocouples locations (in mm over the grate).

The feedstock is introduced from the top using a feeding screw while the oxidizer gas mixture is introduced from the bottom section. The exhaust gas exiting the reactor at the top section is sampled and passed through a heated line to an FTIR analyzer and then after condensation of its water content, to an O<sub>2</sub> analyzer. The FTIR analyzer (Gasmeter DX-4000) has a 0.4 L volume cell with a 5 m pathlength and an 8 cm<sup>−1</sup> resolution. It monitors major and minor species of interest including water vapor and used a factory-set calibration setup specifically designed for high CO<sub>2</sub> (up to 85%) and high water vapor (up to 50%) concentrations. Two calibration series are used for CO, one at ppm level and the other at low% level. The O<sub>2</sub> analyzer is of paramagnetic type, which has a better accuracy and utilization range than the built-in zirconium cell found in the FTIR instrument.

Up to total gas flow rates of approximately 290 NL/min (at 1000 °C), the reactor flow is laminar. The Reynolds number is approximately 1200–1300 for the gas flow rates of interest in this study (160–170 NL/min). The residence time in the reactor is estimated to be ca. 1.6 s. in the heated and insulated zone for gas flow rates of 150–170 NL/min at 1000 °C. The pressure was measured at the top and the bottom of the reactor tube to detect any blockage. Ash samples are collected at the end of each day. The experimental reproducibility has been investigated and is good.

## 2.2. Materials/Feedstocks

One feedstock is used in this study: model MSW pellets.

MSW is a complex, changing, heterogeneous mixture made of a variety of materials, i.e., food, paper, plastic, woody, and non-woody biomass, textiles, metal, glass, and more. Each material can be divided into sub-fractions, e.g., the plastic fraction is made of HDPE (high density polyethylene), PVC (polyvinylchloride), PE (polyethylene), PS (polystyrene), etc. In this study, it is deemed essential to have a good control over the fuel properties while realistically portraying the main characteristics of MSW. After careful consideration, the following mixture (or model MSW) was selected: 10 wt% cardboard (packaging box), 40 wt% virgin wood (from wood pellets) and 50 wt% white office paper, with the overall properties listed in Table 1. The resulting mixture exhibits an elemental composition close to many western-type MSW [3]. It is a simplified MSW, but correctly reflects the main aspects of MSW, most importantly, moderate energy content (less than 20 MJ/kg) and high ash content (above 5 wt%).

**Table 1.** Model MSW pellets main characteristics (EN method).

Properties	Model MSW	Unit
Moisture	3.0	wt% a.s. <sup>2</sup>
Ash content	11.3	wt% a.s. <sup>2</sup>
Volatile matter	78.9	wt% a.s. <sup>2</sup>
S <sup>1</sup>	0.032	wt% d.b. <sup>3</sup>
Cl <sup>1</sup>	0.089	wt% d.b. <sup>3</sup>
C <sup>1</sup>	42.8	wt% d.b. <sup>3</sup>
H <sup>1</sup>	5.4	wt% d.b. <sup>3</sup>
N <sup>1</sup>	0.12	wt% d.b. <sup>3</sup>
O <sup>1</sup>	39.9	wt% d.b. <sup>3</sup>
Calorific value	15.8	MJ/kg d.b.
Dimensions	(6/15)	cm

<sup>1</sup> calculated based on individual constituents' elemental analysis; <sup>2</sup> % weight as received; <sup>3</sup> % weight dry basis.

Plastic (less than 10–12 wt% in most EU MSW) was not included due to the risk of melting on the grate that could damage the reactor. Furthermore, increasing material recycling rates will soon reduce its content in MSW going to WtE.

Biodegradable waste (e.g., food) was not included to avoid hygienic issues during storage and handling of the model MSW. However, it is represented by wood in the model MSW. Like plastic, food waste (in the EU) will be increasingly sorted out for separate treatment (or collected separately) to fulfill EU material recovery rates targets.

Metal and glass were not used as they mainly act as heat sinks (even though melting might happen, for example, for aluminium).

The model MSW is prepared by shredding the various constituents to approximately 5–6 mm particles before mixing them thoroughly (including wetting to ease blending and pelletizing) at the pre-defined proportions. The resulting mixture is then pelletized before being dried to approximately 3–5 wt% moisture content.

### 2.3. Practical Comments on the Set-Up: Feeding System and Changing Operational Conditions

The screw used for fuel feeding had a direct impact on the overall appearance of the emissions trace that exhibited what can be described as small oscillations or variations. The feeding system employed resulted in a kind of “pulsed” (rather than continuous) introduction of pellets, dropping 1–3 at a time before a pause of up to a few seconds depending on the feeding rate. In addition, it was observed that the screw sometime broke pellets while feeding. These phenomena were responsible for minor and random variations but did not have any effect on the validity of the results that are presented as average values. Note that this comment does not apply to large emissions peaks observed when operating conditions are changed and that are due to other processes, e.g., a transient, unstable combustion process.

Furthermore, two distinct events lead to unstable conditions: (a) experiment start-up, as it takes a few minutes for the process to stabilize when feedstock is first introduced, and (b) when changing experimental conditions.

### 2.4. Method/Procedure and General Comments on the Experiments

The overall procedure of an experiment follows these steps (see Figure 1):

- The reactor is heated overnight and left to stabilize at a given reactor temperature, typically 1000 °C. A moderate flow of air is maintained.
- The reactor is operated continuously at a defined fuel effect (i.e., fuel feeding rate), typically 1.3 kg/h, via a screw feeder placed at the top of the VTF furnace.
- The oxidizer mixture (air, N<sub>2</sub> or CO<sub>2</sub> with various O<sub>2</sub> concentration) reaches the grate and the feedstock from below (typical total gas flow rate in: 150–300 NL/min).
- Temperatures (3 thermocouples are placed inside the reactor (see Figure 1); pressure difference (between reactor top and bottom) and gas emissions (exiting from the top of the reactor to an FTIR) are measured and recorded continuously.
- Each experimental period (time during which all parameters are kept constant) lasts from approx. 45 min to approx. 2 h.

The key parameters and variables in this study (experimental matrix in next section):

- Feedstock—model MSW.
- Fuel feeding rate—fixed at 1.3 kg/h.
- Reactor temperature (electrically controlled)—fixed at 1000 °C.
- Oxidizer/gas mass flow rate in—varying or fixed.
- O<sub>2</sub> concentration—varying from 21 to 30 vol%.
- Oxidizer composition—CO<sub>2</sub> or N<sub>2</sub> together with varying O<sub>2</sub> concentrations.

The main experimental results investigated in this study:

- Combustion quality and stability:
  - CO and UHC (unburned hydrocarbons) as main indicators.
  - Temperatures inside the reactor (3 thermocouples (TC) along the VTF).
  - O<sub>2</sub> and CO<sub>2</sub> in exhaust.
- Gaseous pollutants emissions:
  - NO<sub>x</sub> emissions.



The calculated carbon mass balance was satisfying for the experiments, on average 100–120%. Deviations may be due imperfect waste fractions mix in the pellets, varying moisture content (the pellets were not stored under controlled humidity conditions), and analysis limitations, e.g., varying logging time.

The Results and Discussion section provides a concise and precise description of the experimental results, their interpretation and comparison with relevant literature, as well as the conclusions that can be drawn from them.

### 3. Results and Discussion

#### 3.1. The Experimental Matrix and Main Averaged Results

Tables 2 and 3 present the experimental conditions and the main averaged results. Gaseous emissions are normalized (mg/Nm<sup>3</sup>, dry basis, 11% O<sub>2</sub>).

**Table 2.** Varying O<sub>2</sub>/CO<sub>2</sub> concentrations, fixed total flow rate. Feedstock effect: 1.3 kg/h; reactor temperature set at 1000 °C.

Air in (NL/min)	O <sub>2</sub> in (NL/min)	CO <sub>2</sub> in (NL/min)	Sum Gas in (NL/min)	O <sub>2</sub> in (vol%)	NO (mg/Nm <sup>3</sup> )	CO (mg/Nm <sup>3</sup> )	T+287 (°C)
0.0	33.6	126.4	160.0	21.0	133	17	941
0.0	36.8	123.2	160.0	23.0	181	18	963
0.0	40.0	120.0	160.0	25.0	208	21	966
0.0	44.0	116.0	160.0	27.5	314	27	990
0.0	45.0	105.0	150.0	30.0	333	24	997

**Table 3.** Varying O<sub>2</sub>/N<sub>2</sub> concentrations, fixed total flow rate. Feedstock effect: 1.3 kg/h; reactor temperature set at 1000 °C.

O <sub>2</sub> in (NL/min)	N <sub>2</sub> in (NL/min)	CO <sub>2</sub> in (NL/min)	Sum Gas in (NL/min)	O <sub>2</sub> in (vol%)	NO (mg/Nm <sup>3</sup> )	CO (mg/Nm <sup>3</sup> )	T+287 (°C)
36.8	123.2	0.0	160.0	23.0	165	9	1053
40.0	120.0	0.0	160.0	25.0	194	9	1057
44.0	116.0	0.0	160.0	27.5	222	9	1047
48.0	112.0	0.0	160.0	30.0	267	9	1044
33.6	126.4	0.0	160.0	21.0	127	7	1045
40.0	0.0	120.0	160.0	25.0	191	24	980

#### 3.2. Combustion Quality and Stability

##### 3.2.1. Heat and Temperature

The reactor is operated at a temperature of 1000 °C (electrically maintained), which is representative of average combustion temperatures found in the waste bed on air-fired MSW grate incinerators. There are several temperature measurement stations as described in Section 2.1, three of which are placed inside the combustion zone (see Figure 1).

In Figure 2, one can observe the effect of parameters such as oxidizer flow velocity on the reactor behavior, where at higher flow velocity the temperature fluctuates considerably, a sign that the combustion process is affected by intermittent quenching due to a higher equivalence ratio and possibly turbulence effect. The largest fluctuations occur near the grate, where the combustion is starting, but is felt all along the reactor. Note also that the oxidizer gas is injected at the bottom of the reactor at room temperature and the distance to the grate is too short for the oxidizer to reach 1000 °C at the grate's level. The time series shows that the highest fluctuations tendency is observed with a combination of low reactivity oxidizer (i.e., CO<sub>2</sub> as inert and low O<sub>2</sub> concentration) and high velocity, where the temperature is highly unstable (see case 23.7% O<sub>2</sub> in CO<sub>2</sub> at 197 NL/min). An extensive screening has been performed to define an optimal operating range of flow velocity for the cases of interest, which all need to be within cold flow laminar conditions. These tests show that it is important that the temperature measurements are discussed in correlation with the electric power applied to maintain the temperature in the reactor.

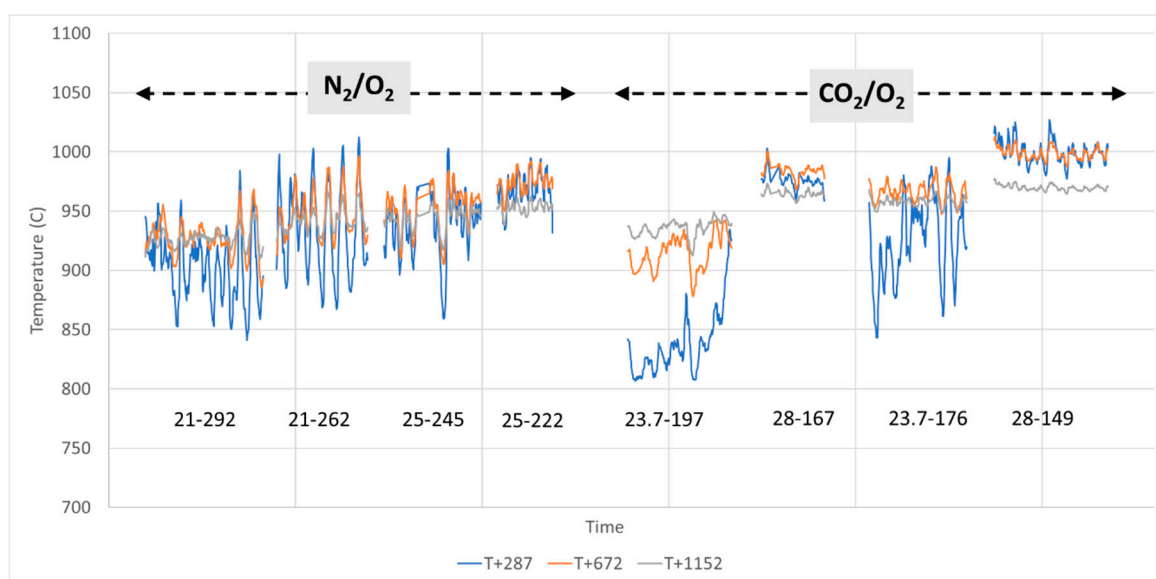


**Figure 2.** Temperature time trace examples (e.g., T+287 = thermocouple placed 287 mm above the grate, see Figure 1) for different oxidizers as specified under each time segment (e.g., first segment on the left is 21% O<sub>2</sub> in N<sub>2</sub> at a flow rate of 292 NL/min).

By operating the reactor without combustion and only air flowing, it was measured that the heat losses through the wall at 1000 °C and the necessary water cooling of flanges are approximately 4 kW. When the fuel is fed into the reactor and combustion initiates, the heat released from combustion can be calculated to be around 6 kW independently of the oxidizer composition tested, which is in agreement with the feeding rate of MSW pellets (1.3 kg/h equivalent to 20.5 MJ/h or 5.7 kW).

Figure 3 shows the reactor temperatures at different O<sub>2</sub> concentrations with N<sub>2</sub> in oxidizer. The heat release occurs mostly near the grate as the highest temperatures are observed at the station closest to the grate “T+287”, i.e., the thermocouple located 28.7 cm above the grate while the electric heater nearest to the grate (“Power bottom”) delivers the lowest power, as shown in Figure 4. The top electrical heater (“Power top”) delivers the highest output to keep the top section of the reactor at 1000 °C to compensate for heat losses. The pattern is rather insensitive to oxygen concentration, apart from a natural tendency for less electrical heating when oxygen concentration increases due to higher heat release at the bottom of the reactor.

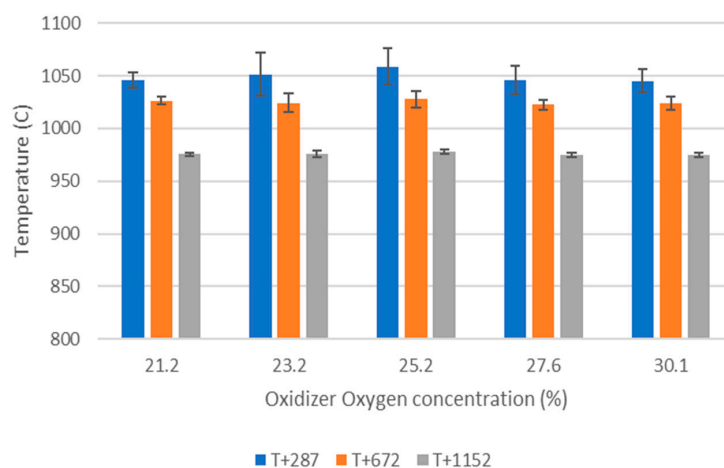


**Figure 3.** Temperatures at different O<sub>2</sub> input concentrations, O<sub>2</sub>/N<sub>2</sub> input mixes, total oxidizer flow rate in: 160 NL/min (except 30.1 case, 150 NL/min). “T+number” indicates the location of the thermocouple above the grate in mm (see also Figure 1).

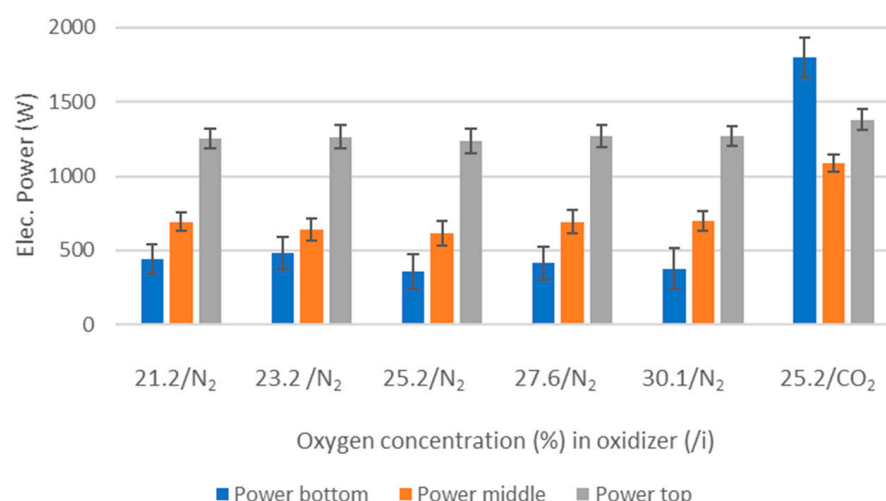


**Figure 4.** Electrical power and O<sub>2</sub> input concentrations, O<sub>2</sub>/N<sub>2</sub> and O<sub>2</sub>/CO<sub>2</sub> input mixes, total oxidizer flow rate in: 160 NL/min (except 30.1 case, 150 NL/min). Power bottom is closest to grate.

When the oxidizer is composed of CO<sub>2</sub> instead of N<sub>2</sub>, the situation in the reactor is affected negatively. To sustain combustion, larger electrical heating is needed as shown in Figure 4, where at 25.2% O<sub>2</sub> in CO<sub>2</sub> the total electric heating applied is twice as much as in the N<sub>2</sub> case. This can be directly related to CO<sub>2</sub> and N<sub>2</sub> different heat capacities. At room temperature, CO<sub>2</sub> has a heat capacity of about 37 J/(mol·K) while N<sub>2</sub>'s is only about 29. Furthermore, the electrical heating is needed mostly at the bottom of the grate, indicating that the combustion heat release is low in that section. The reactor temperatures shown in Figure 5 are indeed highest at the mid-section and barely reaching 1000 °C, even at 30% O<sub>2</sub> in N<sub>2</sub>. The error bars for the temperature at T+287 showing the amplitude of fluctuations (i.e., root mean square) are high, meaning that all the combustion steps (devolatilization, gasification, oxidation) occurring as the MSW pellets fall on the grate are more intermittent and generally less stable. Only the case at 30% O<sub>2</sub> in CO<sub>2</sub> gives temperature distribution in the reactor similar to the air case. A result in accordance with observations made with oxyfuel combustion of coal [9].

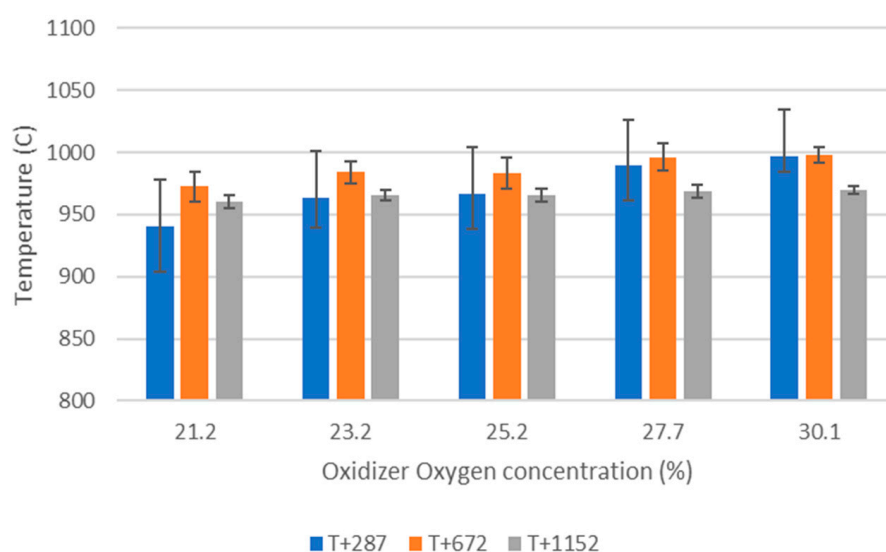


**Figure 5.** Temperatures and O<sub>2</sub> input concentrations, O<sub>2</sub>/CO<sub>2</sub> input mixes, total oxidizer flow rate in: 160 NL/min (except 30.1, 150 NL/min). “T+number”: see Figure 3 caption.



### 3.2.2. CO (+CH<sub>4</sub>, Hydrocarbons)

CO is the main indicator of the combustion process quality (full oxidation) and stability. Poor combustion conditions, especially local reducing conditions due to, e.g., inadequate mixing between fuel and oxidizer or cold spots will lead to (often short-lived) CO peaks. As such, its emission levels are regulated for incineration of MSW. As a reference, the CO BAT-AEL (best available technologies associated emission levels) is 10–50 mg/Nm<sup>3</sup> for new and existing WtE plants (daily average) [3].

For all the model MSW experiments carried out under a variety of conditions (see Section 3.1), stable combustion is achieved with low average levels of CO (below 35 mg/Nm<sup>3</sup>) and none or extremely few individual peaks, occurring mainly when conditions are changed (removed for averaged values). Figures 6 and 7 show the standardized, average CO emissions during model MSW combustion at various O<sub>2</sub> concentrations and mixtures (alternatively N<sub>2</sub> and CO<sub>2</sub>). Overall: (1) CO emissions are slightly higher with CO<sub>2</sub> than N<sub>2</sub> (but still extremely low), (2) CO emissions variations (given as standard deviation) seems to be larger with CO<sub>2</sub> than with N<sub>2</sub>, and (3) these variations seem to be increasing in magnitude with increasing O<sub>2</sub> concentrations (clearly noticeable for O<sub>2</sub>/CO<sub>2</sub>), but acceptable combustion conditions are still attained for all the cases studied.

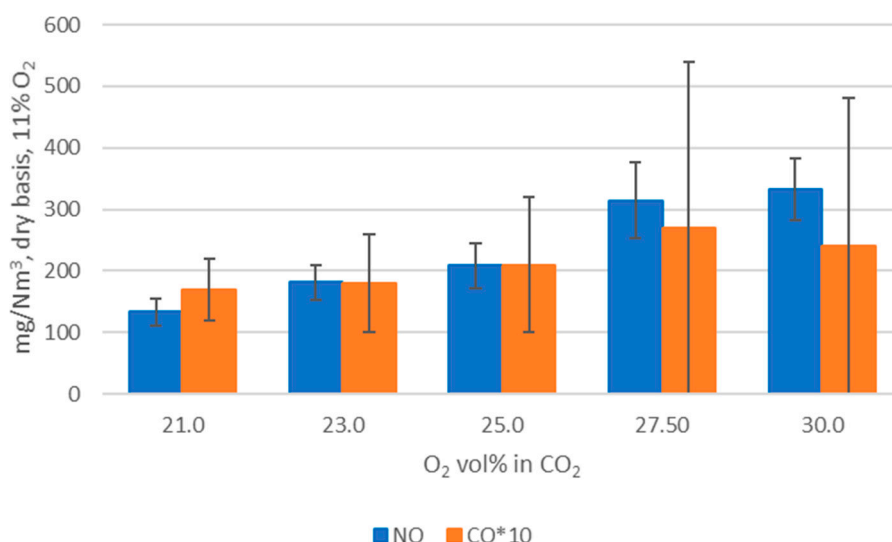


**Figure 6.** NO and CO emissions (with standard deviation) with different O<sub>2</sub>/CO<sub>2</sub> oxidizer mix.

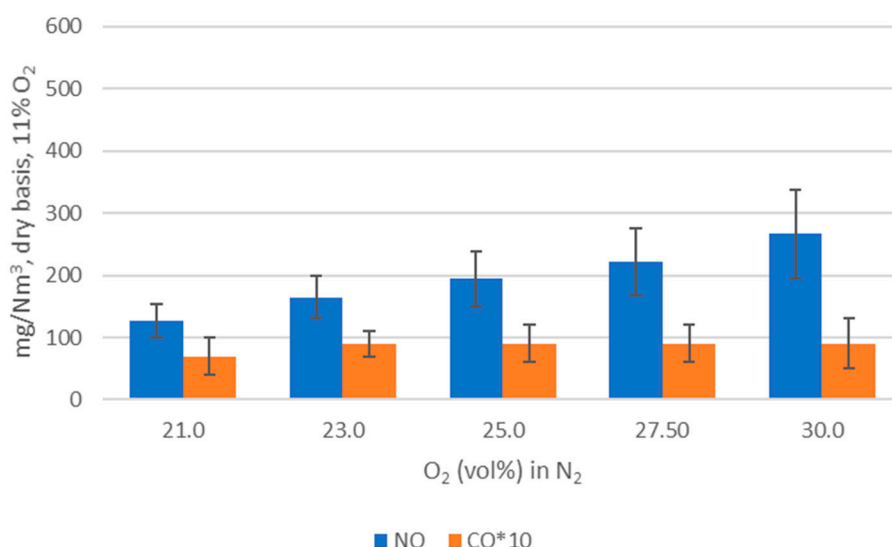


**Figure 7.** NO and CO emissions (with standard deviation) with different O<sub>2</sub>/N<sub>2</sub> oxidizer mix.

The overall conclusion is that our experimental results show the potential offered by oxyfuel combustion of MSW: the model MSW, under different stoichiometries and residence times, O<sub>2</sub> concentrations (ranging from 21 to 30 vol%) in both CO<sub>2</sub> and N<sub>2</sub>, can be properly combusted at similar, low levels of CO, although there is a clear tendency for higher CO values with CO<sub>2</sub> in the oxidizer. As an example, at similar O<sub>2</sub> concentration (25 vol%) and overall conditions, CO concentration and oscillations are approximately 3 times higher with CO<sub>2</sub> than with N<sub>2</sub>. This detrimental effect of CO<sub>2</sub>—also discussed in Section 3.2—on the combustion process agrees with the literature on oxyfuel combustion for coal, where it has been shown that CO<sub>2</sub> can have a strong impact on ignition, flame stability, and char combustion (see Introduction), mainly because of its higher heat capacity compared with N<sub>2</sub>.

The hydrocarbons measured by FTIR analysis (i.e., CH<sub>4</sub>, C<sub>2</sub>H<sub>6</sub>, C<sub>2</sub>H<sub>4</sub>, C<sub>3</sub>H<sub>8</sub>, C<sub>6</sub>H<sub>14</sub>) are found at extremely low levels (1–3 ppm at the most) except in specific instances, especially daily start-up and usually for less than 1 min, confirming the complete combustion in all oxidizer compositions investigated.

### 3.2.3. O<sub>2</sub> and CO<sub>2</sub> in Exhaust Gas

Industrial, full-scale WtE plants must operate with excess air due to the process instabilities (mainly associated with MSW heterogeneity and changing properties), resulting typically in 5–6 vol% O<sub>2</sub> in exhaust gas (wet basis) corresponding to 40% excess air ratio [16], although it is not unusual for older plants to operate at 8–10 vol% O<sub>2</sub>. Operating at as low as possible excess air while ensuring satisfyingly low CO emissions offer several advantages, among others lowering NO<sub>x</sub> production and reducing heat losses due to unused air (mainly N<sub>2</sub>) in the system. It has been shown that it is possible to operate WtE plants with 3 vol% O<sub>2</sub> in the exhaust gas (lambda below 1.20) [16]. In our work, optimal excess air operation was not the main concern. Only a single primary air supply is used, and hence mixing between fuel and oxidizer is probably not optimal and limited by the set-up configuration (fixed grate, tube reactor, cold oxidizer, gas pre-mixing, and distribution). Under acceptable conditions with air, the reactor operated with 5–10 vol% O<sub>2</sub> in the exhaust (wet basis) corresponding to lambda of 1.5+. Optimizing air excess ratio and oxidizer addition supply strategy will be necessary when further developing MSW oxyfuel combustion.

For the experiments using CO<sub>2</sub> in the oxidizer (see Table 2), CO<sub>2</sub> concentrations in the exhaust gas vary between 78.5 and 86.6 vol% (wet basis), while with N<sub>2</sub> in the oxidizer (See Table 3), CO<sub>2</sub> concentrations are approximately 10–11 vol% (wet basis). Higher CO<sub>2</sub> concentrations are an important factor facilitating CCS. The ability to carry out a stable and complete combustion process for MSW in CO<sub>2</sub> rather than N<sub>2</sub> as demonstrated in this study is an important step in the development of oxyfuel combustion as a viable CCS route for WtE.

### 3.3. NO<sub>x</sub> (NO, NO<sub>2</sub>), N<sub>2</sub>O and Other Gaseous Pollutants

In the EU, several emissions to air from WtE are regulated. This includes dust, metals, metalloids, mercury, HCl, HF, SO<sub>2</sub>, NH<sub>3</sub>, and organic compounds (dioxins, furans, PCBs). In addition to the main combustion products, our FTIR (see Section 2.1) is calibrated to measure HCl, HF, SO<sub>2</sub>, HCN, and NH<sub>3</sub> online. Minute levels of the aforementioned species (1–2 ppm) were detected during the experiments. It is to be expected as the model MSW has low levels of S and Cl. Oxyfuel combustion will not create new challenges regarding these pollutants and it is expected that they will be handled as with air combustion as the same fundamental chemical processes can be expected below 1500 °C.

NO<sub>x</sub> is highly sensitive to temperature and O<sub>2</sub> availability, two parameters affected by oxyfuel combustion compared with air combustion. In MSW incineration, NO<sub>x</sub> is overwhelmingly formed via the fuel NO<sub>x</sub> mechanism where HCN and NH<sub>3</sub> released from the feedstock are oxidized to NO [17]. A lack of oxidizer will hence limit fuel-NO<sub>x</sub> formation. Thermal NO<sub>x</sub>, and even more so prompt NO<sub>x</sub>, are not expected to play an

important role in air-fired MSW grate incineration. Temperature control (using recirculated flue gas) with oxyfuel combustion of MSW should ensure that fuel  $\text{NO}_x$  remains the only  $\text{NO}_x$  forming mechanism. Our experiments show the intertwined influence of turbulence, temperature and  $\text{O}_2$  availability on  $\text{NO}_x$  formation during oxyfuel combustion.

The experiments show that  $\text{NO}$  emissions increase with increasing  $\text{O}_2$  concentrations, (see Figures 6–8 and Tables 2 and 3). Only minute amounts of  $\text{NO}_2$  and  $\text{N}_2\text{O}$  are detected. Increasing from 21 to 30 vol%  $\text{O}_2$ , the normalized  $\text{NO}_x$  emissions are more than doubled. This confirms that  $\text{O}$  availability is paramount to  $\text{NO}_x$  formation in the system studied. While  $\text{NO}_x$  emissions are often reported to decrease (on energy basis) in an oxy-combustion system with coal [10], the  $\text{NO}_x$  concentration in the exhaust gas is usually similar or higher than with air combustion [11]. Most oxy-combustion studies concerning waste and biomass are limited to TGA kinetics studies of biomass residues and individual waste fractions, but the increasing and stabilizing  $\text{NO}_x$  trend observed here is in accordance with the existing literature [18], even though the actual emissions levels will be strongly dependent on the fuel and the operating conditions. There are no significant differences between experiments with  $\text{N}_2$  and  $\text{CO}_2$  at 21–25  $\text{O}_2$  vol%, but  $\text{NO}_x$  emissions seem a bit higher in  $\text{CO}_2$  above this point and reach a plateau at approx. 250–350  $\text{mg}/\text{Nm}^3$ . The  $\text{CO}_2$  thermal properties (higher heat capacity than  $\text{N}_2$ ) are not affecting  $\text{NO}_x$  formation when compared at equal  $\text{O}_2$  concentration because the reactor is set at a constant temperature; therefore, the lower combustion temperature with  $\text{CO}_2$  is compensated by higher electrical heating (see Section 3.2.1). Thus, in Figure 8, the thermal effect on  $\text{NO}$  formation is decoupled from the chemical effect of oxygen and it allows to conclude that  $\text{CO}_2$  is not chemically involved in the formation of  $\text{NO}_x$  in this temperature range. There could also be an additional effect due to increased local turbulence (and hence better gas phase mixing) when shifting from  $\text{N}_2$  to  $\text{CO}_2$  as suggested by the more unstable  $\text{CO}$  emissions.

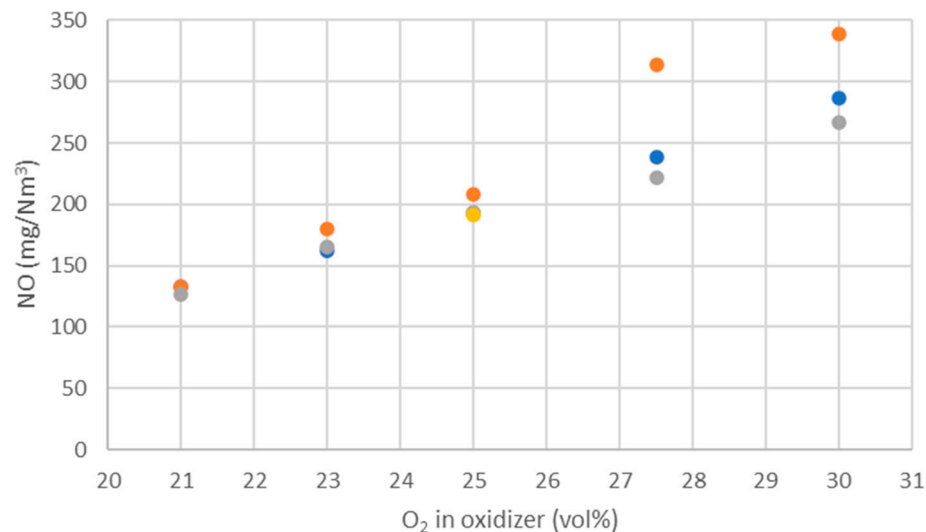


**Figure 8.**  $\text{NO}_x$  emissions as a function of  $\text{O}_2$  input concentration.  $\text{O}_2/\text{CO}_2$  (orange and yellow) and  $\text{O}_2/\text{N}_2$  (blue and grey) mixtures. Similar conditions (1000 °C, 1.3 kg/h, 160 NL/min (except the highest point at 30%, 150 NL/min)).

Even though the results obtained in this laboratory scale set-up cannot be directly extrapolated to an industrial grate furnace, they represent the chemical phenomena where combustion takes place, and  $\text{NO}$  formation occurs. Comparing the propensity of  $\text{NO}$  to form in air and oxyfuel mode allows to predict that  $\text{NO}_x$  should not be a major issue. Therefore, similar  $\text{NO}_x$  reduction measures (primary and/or secondary) as in conventional plant should be sufficient. The higher concentrations obtained if the local  $\text{O}_2$  concentrations are purposely selected higher (to achieve for example higher local temperature or higher

heat release rate) could lead to higher  $\text{NO}_x$  concentration in the flue gas and to higher reduction costs; however, the reduced flue gas volume could compensate that effect.

### 3.4. Important Considerations for a Full-Scale MSW Oxyfuel Combustion Plant

An important aspect that should not be neglected even at the early stages of MSW oxyfuel combustion development is the question of legislation and operation permit. Oxyfuel combustion may be considered significantly different from air combustion and several aspects (e.g., residence time, temperature, flue gas amounts, emissions levels) may require new / revised legislation and a new kind of operation permit. This is most certainly a time-consuming and uncertain undertaking. Risks and uncertainties can be reduced if the system proposed remains similar to traditional grate-fired incineration, as we strongly recommend.

We believe that for optimal implementation of (1) oxyfuel combustion for proper destruction of contaminants in non-recyclable MSW, (2) heat/power production, (3) efficient flue gas cleaning, and (4) carbon capture, new plants especially designed are the preferred option. The best overall approach would be to remain as close as possible to the existing air-fired grate installations in terms of design, processes, technologies, and materials. Even though savings in terms of equipment size can be expected, additional costs for  $\text{O}_2$  production, temperature monitoring, and control may be necessary (and possibly the need for secondary  $\text{NO}_x$  reduction measures). The example of the SYNCOM technology [19] shows the advantages and challenges observed in a grate system at low / intermediate levels of oxygen enrichment.

## 4. Conclusions

WtE with advanced gas cleaning system destroys contaminants and reduces the weight and volume of mixed waste that cannot be recycled. It also produces mainly renewable energy as MSW is predominantly of biogenic origin. Combined with CCS, WtE would hence offer the potential for carbon negative emissions, a key measure to fight climate change. Several CCS technologies exist or are under development and oxyfuel combustion integrated with CCS has shown to be a promising technology for solid fuels such as coal. The experimental assessment of oxyfuel combustion in a laboratory scale reactor performed and reported in this study shows that a model MSW can satisfactorily be combusted under different oxyfuel conditions provided that the oxygen concentration in the oxidizer is carefully adapted. The results also indicate that there is no unsurmountable showstopper for the further development of MSW oxyfuel combustion. The results in this study contribute to the further development of oxyfuel combustion as they confirm that stable combustion can be attained under different operating oxyfuel conditions, using both  $\text{N}_2$  and  $\text{CO}_2$ , for a complex mixture. Stable combustion with high  $\text{CO}_2$  concentrations (in the range of 78–87 vol% in the flue gas) was attained even though  $\text{CO}_2$ 's higher heat capacity (compared with  $\text{N}_2$ ) impacts the combustion process negatively. Working at these conditions will greatly facilitate the implementation of  $\text{CO}_2$  capture. The results also indicate that  $\text{NO}_x$  emissions will be increasing with O availability, a trend observed both with  $\text{N}_2$  and  $\text{CO}_2$ .

The aforementioned challenges can be addressed, e.g., with adequate combustion chamber design, appropriate local  $\text{O}_2$  concentrations, advanced recirculated flue gas strategy (amount, temperature, wet/dry, raw/clean), and primary and secondary measures for  $\text{NO}_x$ . Further oxyfuel combustion development should be considered in the perspective of a system building upon air-fired grate combustion technology with combustion temperatures below 1200 °C to benefit from the existing know-how while avoiding excessive material costs. This is especially important to be able to handle untreated, mixed, unrecyclable waste.

Further studies should advance further oxyfuel combustion and include experiments with higher  $\text{O}_2$  concentrations, (bottom and fly) ash analysis, other waste mixtures, kinetics, different reactor temperatures, study of local conditions, and the effects of heterogeneity,

temperature measurements in a waste bed under oxyfuel conditions, advanced oxidizer supply strategies, and optical study to observe the combustion process in situ.

**Author Contributions:** Conceptualization, M.D., M.B., P.C., J.B., J.S. and M.N.P.O.; investigation, J.B. and M.N.P.O.; data curation, M.B., M.D. and J.B.; writing—original draft preparation, M.B. and M.D.; writing—review and editing, J.B., P.C., J.S. and M.N.P.O.; project administration, M.D. and J.S.; funding acquisition, M.D. and J.S. All authors have read and agreed to the published version of the manuscript.

**Funding:** The research was funded by the Research Council of Norway (RCN) through the Cape-Waste IPN project (grant number 281869) and the ERA NET Cofund ACT NEWEST-CCUS project (grant number 305062).

**Data Availability Statement:** Restrictions apply to the availability of these data.

**Conflicts of Interest:** The authors declare no conflict of interest. The funders had no role in the design of the study; in the collection, analyses, or interpretation of data; in the writing of the manuscript, or in the decision to publish the results.

## References

1. Stuen, J. CCS from Waste Incineration from Polluting Industry to Part of the Climate Solution. 2019. Available online: <https://www.forskningsradet.no/contentassets/3fb0ac44a9c5479f8aca0fb12eadd133/johnny-stuen-fortum-oslo-varme-klemetsrud-energi-gjenvinningsanlegg-med-ccs-efk2019-.pdf> (accessed on 20 August 2021).
2. IPCC Special Report. Global Warming of 1.5 °C. 2018. Available online: <https://www.ipcc.ch/sr15/> (accessed on 20 August 2021).
3. JRC Science for Policy Report. BAT Reference Document for Waste Incineration. 2019. Available online: <https://eippcb.jrc.ec.europa.eu/reference/Waste-incineration-0> (accessed on 20 August 2021).
4. Fagerlund, J.; Zevenhoven, R.; Thomassen, J.; Tednes, M.; Abdollahi, F.; Thomas, L.; Nielsen, C.J.; Mikoviny, T.; Wisthaler, A.; Zhu, L.; et al. Performance of an amine-based CO<sub>2</sub> capture pilot plant at the Fortum Oslo Varme Waste to Energy plant in Oslo, Norway, 2021. *Int. J. Greenh. Gas Control.* **2021**, *106*, 103242. [CrossRef]
5. Stanger, R.; Wall, T.; Spörl, R.; Paneru, M.; Grathwohl, S.; Weidmann, M.; Scheffknecht, G.; McDonald, D.; Myöhänen, K.; Ritvanen, J.; et al. Oxyfuel combustion for CO<sub>2</sub> capture in power plants. *Int. J. Greenh. Gas Control.* **2015**, *40*, 55–125. [CrossRef]
6. Baukal, C.E., Jr. *Oxygen-Enhanced Combustion*; CRC Press: Boca Raton, FL, USA, 2013; ISBN 0-8493-1695-2 (1998).
7. Al-Makhadmeh, L.; Maier, J.; Scheffknecht, G. Coal pyrolysis and char combustion under oxyfuel conditions. In Proceedings of the 34th International Technical Conference on Clean Coal & Fuel Systems, Clearwater, FL, USA, 31 May–4 June 2009; pp. 112–123.
8. Shaddix, R.; Hecht, H.; Jimenez, S.; Lee, S. Evaluation of rank effects and gas temperature on coal char burning rates during oxyfuel combustion. In Proceedings of the 34th International Technical Conference on Clean Coal & Fuel Systems, Clearwater, FL, USA, 31 May–4 June 2009.
9. Grathwohl, S.; Maier, J.; Scheffknecht, G. Testing and Evaluation of Advanced Oxyfuel Burner and Firing Concepts. In Proceedings of the 2nd Oxyfuel Combustion Conference (OCC2), Yeppoon, Australia, 12–16 September 2011.
10. Buhre, B.J.; Elliott, L.K.; Sheng, C.; Gupta, R.P.; Wall, T.F. Oxyfuel combustion technology for coal-fired power generation. *Prog. Energy Combust. Sci.* **2005**, *31*, 283–307. [CrossRef]
11. Ramos, J.; Navarrete, B.; Munoz, F.; Gil, B.; Otero, P.; Kuivalainen, R.; Hiltunen, T. NO<sub>x</sub> emissions experiences in a 30MWth circulating fluidized bed boiler under oxy-combustion conditions. In Proceedings of the 3rd Oxyfuel Combustion Conference (OCC3), Ponferrada, Spain, 9–13 September 2013.
12. Wienchol, P.; Szlęk, A.; Ditaranto, M. Waste-to-energy technology integrated with carbon capture—Challenges and opportunities. *Energy* **2020**, *198*, 117352. [CrossRef]
13. Tang, Y.; Ma, X.; Lai, Z.; Fan, Y. Thermogravimetric analyses of co-combustion of plastic, rubber, leather in N<sub>2</sub>/O<sub>2</sub> and CO<sub>2</sub>/O<sub>2</sub> atmospheres. *Energy* **2015**, *90*, 1066–1074. [CrossRef]
14. Shah, I.A.; Gou, X.; Zhang, Q.; Wu, J.; Wang, E.; Liu, Y. Experimental study on NO<sub>x</sub> emission characteristics of oxy-biomass combustion. *J. Clean. Prod.* **2018**, *199*, 400–410. [CrossRef]
15. Sher, F.; Pans, M.A.; Sun, C.; Snape, C.; Liu, H. Oxy-fuel combustion study of biomass fuels in a 20 kWth fluidized bed combustor. *Fuel* **2018**, *215*, 778–786. [CrossRef]
16. Strobel, R.; Waldner, M.H.; Gablinger, H. Highly efficient combustion with low excess air in a modern energy from-waste (EfW) plant. *Waste Manag.* **2018**, *73*, 301–306. [CrossRef] [PubMed]
17. Becidan, M.; Skreiberg, Ø.; Hustad, J.E. NO<sub>x</sub> and N<sub>2</sub>O Precursors (NH<sub>3</sub> and HCN) in Pyrolysis of Biomass Residues. *Energy Fuels* **2007**, *21*, 1173–1180. [CrossRef]

- 
18. Tang, Y.; Ma, X.; Lai, Z.; Zhou, D.; Lin, H.; Chen, Y. NO<sub>x</sub> and SO<sub>2</sub> emissions from municipal solid waste (MSW) combustion in CO<sub>2</sub>/O<sub>2</sub> atmosphere. *Energy* **2012**, *40*, 300–306. [[CrossRef](#)]
  19. Martin GmbH Website. Available online: [https://www.martingmbh.de/media/files/Technologie/SYNCOM\\_Plus18.pdf](https://www.martingmbh.de/media/files/Technologie/SYNCOM_Plus18.pdf) (accessed on 20 August 2021).